Published in final edited form as:
Neuron. 2011 February 24; 69(4): 780–792. doi:10.1016/j.neuron.2011.01.016.

Serotonin Mediates Cross-Modal Reorganization of Cortical Circuits

Susumu Jitsuki[1], **Kiwamu Takemoto**[1,2], **Taisuke Kawasaki**[1], **Hirobumi Tada**[1], **Aoi Takahashi**[1], **Carine Becamel**[3], **Akane Sano**[1], **Michisuke Yuzaki**[4], **R. Suzanne Zukin**[5], **Edward B. Ziff**[6], **Helmut W. Kessels**[7], and **Takuya Takahashi**[1,5,8,*]

[1]Yokohama City University Graduate School of Medicine, Department of Physiology, Yokohama 236-0004, Japan

[2]JST, PRESTO, Saitama 332-0012, Japan

[3]Institut de Génomique Fonctionnelle-Dépt. de Neurobiologie, Montpellier 34094, France

[4]Keio University School of Medicine, Department of Physiology, Tokyo 160-8582, Japan

[5]Albert Einstein College of Medicine, Dominick P. Purpura Department of Neuroscience, Bronx, NY 10461, USA

[6]New York University, New York, NY 10016, USA

[7]University of California, San Diego, La Jolla, CA 92093, USA

[8]JST, CREST, Saitama, 332-0012, Japan

SUMMARY

Loss of one type of sensory input can cause improved functionality of other sensory systems. Whereas this form of plasticity, cross-modal plasticity, is well established, the molecular and cellular mechanisms underlying it are still unclear. Here, we show that visual deprivation (VD) increases extracellular serotonin in the juvenile rat barrel cortex. This increase in serotonin levels facilitates synaptic strengthening at layer 4 to layer 2/3 synapses within the barrel cortex. Upon VD, whisker experience leads to trafficking of the AMPA-type glutamate receptors (AMPARs) into these synapses through the activation of ERK and increased phosphorylation of AMPAR subunit GluR1 at the juvenile age when natural whisker experience no longer induces synaptic GluR1 delivery. VD thereby leads to sharpening of the functional whisker-barrel map at layer 2/3. Thus, sensory deprivation of one modality leads to serotonin release in remaining modalities, facilitates GluR1-dependent synaptic strengthening, and refines cortical organization.

INTRODUCTION

In order to receive better information about their external environment, blind individuals compensate their lack of visual input by responding to somatosensory or auditory input with improved sensitivity and accuracy. The brain can adapt to sensory deprivation in one modality (e.g., visual cortex) by increasing plasticity and retuning neuronal circuits in other remaining modalities. Although dynamic cortical reorganization among different sensory

*Correspondence: takahast@yokohama-cu.ac.jp.

SUPPLEMENTAL INFORMATION

Supplemental Information includes Supplemental Experimental Procedures and five figures and can be found with this article online at doi:10.1016/j.neuron.2011.01.016.

areas is critical for this adaptation, the molecular and cellular mechanisms underlying it are still poorly understood (Bavelier and Neville, 2002; Goel et al., 2006; Rauschecker et al., 1992; Sadato et al., 1996).

Neural plasticity is regulated by higher cognitive functions such as mental arousal and attention (Clark and Squire, 1998; Hu et al., 2007; McIntosh et al., 1999). Cross-modal reorganization of different sensory systems may require a coordinated shift of attention from the deprived to the intact sense (Dye et al., 2007; Macaluso and Driver, 2001). Serotonergic neurons originating from the dorsal raphe nucleus widely innervate many brain regions and play a central role in higher cognitive functions such as attention and motivation (Geyer and Vollenweider, 2008; Vertes, 1991). Thus, the serotonergic system could orchestrate cortical reorganization among different sensory systems through the modifications of synaptic plasticity. Although the effect of serotonin on synaptic plasticity such as long-term potentiation (LTP), a cellular model of synaptic plasticity, has been described (Inaba et al., 2009; Kim et al., 2006; Kojic et al., 1997; Normann and Clark, 2005), knowledge about the physiological roles of or the molecular mechanisms behind serotonin-mediated plasticity is lacking.

The majority of excitatory synapses in the mammalian central nervous system use glutamate as a neurotransmitter. Fast glutamatergic transmission is mainly mediated by AMPA (α-amino-3-hydroxy-5-methyl-4-isoxazole propionic acid) type ionotropic glutamate receptors (AMPARs) (Bredt and Nicoll, 2003; Hollmann and Heinemann, 1994). AMPARs are tetramers comprised of a combinatorial assembly of four subunits, GluR1-4 (Mansour et al., 2001; Wenthold et al., 1996). Synaptic plasticity at glutamatergic synapses is considered to be crucial for cognitive functions such as learning and memory. The best-studied form of synaptic plasticity is LTP and its molecular mechanisms have been extensively characterized. Synaptic delivery and addition of AMPARs appears to be a major mechanism regulating post-synaptic expression of LTP (Barry and Ziff, 2002; Bredt and Nicoll, 2003; Hayashi et al., 2000; Malinow and Malenka, 2002; Scannevin and Huganir, 2000; Shi et al., 1999). LTP-inducing stimuli in vitro drive GluR1-containing AMPARs into synapses and enhance synaptic transmission (Hayashi et al., 2000). The same molecular modification occurs during experience-dependent neuronal reorganization in vivo. Sensory experience early in development delivers GluR1 into synapses of the rodent barrel cortex (Clem and Barth, 2006; Takahashi et al., 2003). Fear learning also induces synaptic GluR1 delivery in amygdala (Rumpel et al., 2005).

Here, we present a comprehensive study that explains how visual deprivation (VD) leads to improved whisker function in the rat on a molecular, cellular, and circuit level. We found that VD increased the extracellular serotonin levels in the barrel cortex, thereby facilitating the delivery of GluR1 into layer 4-2/3 synapses. Furthermore, this resulted in a sharpening of the functional whisker-barrel map. Thus, serotonin mediates cross-modal cortical reorganization induced by sensory deprivation through the facilitation of synaptic GluR1 delivery and results in the improvement of remaining sensory functions.

RESULTS

Visual Deprivation Drives GluR1 into Synapses from Layer 4 to Layer 2/3 in the Juvenile Rat Barrel Cortex

As an approach to study cross-modal plasticity, we used techniques to monitor and manipulate synaptic trafficking of AMPARs. Synaptic plasticity models have identified the regulated trafficking of AMPARs that contain the GluR1 subunit into the postsynaptic membrane as a prevalent mechanism underlying activity-induced changes in synaptic transmission (Barry and Ziff, 2002; Bredt and Nicoll, 2003; Kessels and Malinow, 2009). In

young rats (P12–P14), whisker experience is sufficient to drive GluR1-containing AMPARs into layer 4 to 2/3 synapses of the barrel cortex and promotes establishment of the functional whisker-barrel map at layer 2/3 (Takahashi et al., 2003). At later ages (P21–P23), when functional organization of the whisker-barrel map at layer 2/3 is complete (Stern et al., 2001), we expect whisker experience by itself to be insufficient for driving GluR1 into layer 4-2/3 synapses in the barrel cortex. To examine this, we employed an "electrophysiological tagging" technique (Hayashi et al., 2000) to detect synaptic delivery of recombinant GluR1 tagged with a green fluorescent protein (GFP-GluR1). Overexpression of recombinant GFP-GluR1 forms homomeric receptors which, in contrast to the majority of endogenous AMPARs, are inwardly rectifying: they display little outward current at positive membrane potential compared to endogenous receptors. Synaptic localization of recombinant GFP-GluR1 can therefore be determined by measuring the rectification index: the ratio of EPSC amplitude at −60 mV to +40 mV. We microinjected Herpes simplex virus carrying GFP-GluR1 into layer 2/3 of the barrel cortex at P21. 36 hr after injection, acute brain slices were prepared and excitatory synaptic transmission at layer 4 to layer 2/3 synapses was examined by whole-cell recordings from pyramidal neurons (Figure 1A). GFP-GluR1 infected neurons did not display an increase in rectification, indicating natural whisker experience did not drive synaptic delivery of GFP-GluR1 at this age (Figure 1B). To examine whether endogenous GluR1 receptors behave in a manner similar to that of GFP-GluR1 receptors, we expressed a construct encoding GFP-tagged cytoplasmic tail of GluR1 (GFP-GluR1ct), which specifically blocks synaptic potentiation mediated by delivery of endogenous GluR1-containing AMPARs (Shi et al., 2001). No synaptic depression was observed at neurons expressing GFP-GluR1ct (Figure 1C), indicating that, at P21–P23, natural whisker experience no longer induced GluR1-dependent synaptic plasticity at layer 4-2/3 synapses in the barrel cortex.

In order to examine if synaptic GluR1 delivery underlies cortical reorganization induced by VD, we tested the effect of VD on the trafficking of GluR1 at layer 4-2/3 synapses in the barrel cortex at P21–P23. We sutured both eyes immediately after microinjection of virus expressing GFP-GluR1 into the barrel cortex. 36 hr later, we prepared acute brain slices and performed whole-cell recordings from layer 4-2/3 pyramidal synapses. Under these conditions, AMPARs-mediated transmission of GFP-GluR1 expressing neurons exhibited enhanced rectification relative to transmission onto nearby noninfected neurons (Figure 1B), indicating that GFP-GluR1 was incorporated into layer 4-2/3 synapses of the barrel cortex in response to VD. This synaptic GluR1 incorporation was whisker-experience dependent, since average rectification values were unaffected in VD animals whose whiskers were trimmed (Figure 1F).

Next, we tested if VD drives endogenous GluR1-contanining AMPARs into layer 4-2/3 synapses in the barrel cortex. Expression of GFP-GluR1ct (P21–P23) depressed AMPA transmission at synapses of the barrel cortex in animals subjected to VD (P21–P23) (Figure 1C). Furthermore, a higher proportion of neurons in the barrel cortex from VD animals (VD during P21–P23) displayed an increased ratio of AMPA/NMDA EPSC (A/N ratio) at P23, another indicator of synaptic delivery of endogenous AMPARs, compared with those from control animals (Figure 1D; see Figures S1B and S1C available online). In order to further examine if VD (P21–P23) delivers endogenous AMPARs at layer 4-2/3 synapses in the barrel cortex, we replaced extracellular Ca^{2+} with Sr^{2+} to induce asynchronous transmitter release and analyzed quantal EPSCs at layer 4-2/3 synapses in the barrel cortex of either VD or intact animals. We found an increased amplitude of evoked mEPSC at layer 4-2/3 synapses of VD rats than intact animals at P23 (Figure 1G). Two days of VD (P21–P23) also increased rectification at layer 4-2/3 synapses (Figure 1H; Figure S1A). These findings demonstrate that VD leads to the delivery of endogenous GluR1-containing AMPARs at layer 4-2/3 synapses of the barrel cortex. Notably, we did not detect any difference in

rectification values between GFP-GluR1 expressing and nonexpressing pyramidal neurons at layer 2/3 of VD rats when we stimulated the lateral pathway (layer 2/3–layer 2/3 synapses), indicating stable synaptic GFP-GluR1 delivery was absent in synapses that receive their input from the lateral pathway of VD animals (Figure 1E). Thus, VD-driven synaptic GluR1 delivery was confined to the layer 4-2/3 pathway.

While natural whisker experience no longer drives GluR1 into layer 4-2/3 synapses at the juvenile age, VD delivers GluR1 into these synapses, indicating that layer 2/3 neurons in the barrel field are still plastic at this age. It is conceivable that after completion of the construction of functional barrel map (i.e., after P14), plastic changes in the barrel map mainly occur in response to changes in sensory experience (e.g., novel environment or whisker loss). Indeed, manipulations that alter whisker input induce changes in neuronal properties in the barrel field at older ages (Diamond et al., 1994; Holtmaat and Svoboda, 2009). Consistent with the notion that barrel neurons maintain their capacity to generate synaptic plasticity, LTP was successfully induced at layer 4-2/3 synapses at P23 (Figure 2B). However, 2 days after the initiation of VD, GluR1 delivery appeared to have reached saturated amounts of AMPARs at layer 4-2/3 synapses, as induction of LTP at this pathway was occluded by P23 in animals exposed to VD beginning at P21 (Figures 2A and 2B). This effect was unlikely due to changes in synaptic NMDA-receptor content or inhibitory synaptic responses, since we detected no differences in input-output curve of NMDA-receptor EPSCs and IPSCs or in decay kinetics of NMDA-receptors mediated synaptic responses between intact and VD animals (Figure S2). Furthermore, expression of GFP-GluR1 during P23–P25 in the barrel cortex of rats that received VD at P21 did no longer result in alterations in the rectification index at synapses onto GFP-GluR1-expressing neurons (Figure 2C). These data suggest that VD-driven synaptic GluR1 delivery lasts at most 2 days and is closed by 3 days after initiation of VD.

Serotonin Mediates VD-Induced Synaptic GluR1 Delivery

What mediates VD-induced synaptic delivery of GluR1 in the barrel cortex? Previous studies have shown that the serotonergic system plays critical roles in development and functional organization of the barrel cortex (Bennett-Clarke et al., 1994, 1995; Turlejski et al., 1997). Activation of serotonin receptors enhances plasticity at excitatory synapses onto the basolateral region of the amygdala (Chen et al., 2003). Moreover, increase of extracellular serotonin with SSRI (selective serotonin reuptake inhibitor) restores ocular dominance plasticity in the visual cortex after critical period is terminated (Maya Vetencourt et al., 2008). These findings support the notion that serotonin is a major regulator of neural plasticity in the brain. Therefore, we hypothesized that serotonin potentially facilitates GluR1 delivery at layer 4-2/3 synapses in the barrel cortex in response to VD in rats. To examine this possibility, we first measured extracellular serotonin levels in the barrel cortex of rats in the absence or presence of VD by in vivo microdialysis. We sutured both eyes at P21 and performed in vivo microdialysis at P23. We detected increased levels of extracellular serotonin in the barrel cortex of VD animals relative to those of intact rats (Figure 3A). In contrast, exposure to VD did not elicit a significant alteration in extracellular serotoninin the visual cortex (Figure 3A). Furthermore, VD did not detectably alter extracellular dopamine levels in the barrel cortex (Figure 3B). Thus, VD selectively increases extracellular serotonin in the rat barrel cortex.

To examine whether serotonin mediates VD-induced synaptic incorporation of GluR1 in the barrel cortex, we injected ketanserin, a 5HT2A/2C serotonin receptor antagonist, into layer 2/3 of the barrel cortex together with Herpes simplex virus expressing GFP-GluR1 at age P21. Immediately after injection, we induced VD by suturing both eyes and, 36 hr later, prepared acute brain slices from animals aged P23. Whole-cell recording from layer 4 to 2/3 synapses revealed no detectable difference in rectification in infected versus noninfected

pyramidal neurons, indicating no synaptic delivery of GFP-GluR1 (Figure 3C). This finding suggests that VD-induced synaptic GFP-GluR1 delivery is mediated by serotonin. Consistent with this, A/N ratios in neurons of VD animals injected with ketanserin were significantly lower than those of saline-injected VD rats (Figure 3D), suggesting that VD-induced synaptic delivery of endogenous AMPARs is mediated by serotonin.

To determine if serotonin directly modulates intracellular signaling cascades required for synaptic GluR1 delivery, we introduced short hairpin RNA (shRNA) to knock down expression of endogenous 5HT2A receptors (Sh5HT2A) of layer 2/3 pyramidal neurons in the barrel cortex of rats with VD in vivo. Sh5HT2A reduced the expression of endogenous 5HT2A when expressed P15–P23 in vivo and assayed with immunoblotting at P23 (Figure S3A). In order to analyze single isolated neurons, we microinjected low titer lenti virus carrying Sh5HT2A into the barrel cortex at P15. At P21, both eyes were sutured, and acute brain slices were prepared for whole-cell recording at P23. Sh5HT2A expressing neurons (detected by coexpressing GFP) were mainly localized in layer 2/3 (Figure 3E; Figure S3C). We found that Sh5HT2A expressing layer 2/3 neurons exhibited decreased synaptic AMPA transmission compared with nearby uninfected neurons, while neurons expressing scramble construct did not display reduced AMPA transmission (Figure 3E). Furthermore, cointroduction of a 5HT2A receptor that is resistant to the Sh5HT2A hairpin (res-Sh5HT2A) into the barrel cortex could prevent the Sh5HT2A-mediated block of synaptic potentiation after VD induction (Figure 3E). This result indicates that the effect of the Sh5HT2A hairpin is specific to the 5HT2A receptor. Expression of Sh5HT2A did not exhibit any effect on AMPA-mediated transmission in non-VD animals (Figure S3B). These results indicate that 5HT2A receptor expression is required for VD-induced synaptic AMPARs trafficking. Our experiments did not exclude the possibility that besides 5HT2A receptors also 5HT2C receptors were involved in VD-induced plastic changes.

Serotonin Facilitate Synaptic GluR1 Delivery

To examine whether increased serotonin levels are sufficient to facilitate experience-dependent synaptic GluR1 delivery, we first examined whether natural whisker-input could drive GluR1 into synapses when serotonin signaling was artificially enhanced. We injected DOI (2,5-dimethoxy-4-iodoamphetamine), a 5HT2A/2C receptor agonist, together with virus expressing GFP-GluR1 into layer 2/3 of the barrel cortex at P21 in animals with intact vision. We prepared acute brain slices 36 hr after infection and performed whole-cell recording to examine excitatory synaptic transmission at layer 4 to 2/3 pyramidal synapses. We observed increased rectification at synapses onto GFP-GluR1 expressing neurons compared with uninfected neurons, indicating synaptic delivery of GFP-GluR1 (Figure 4A). The A/N ratio in neurons of rats injected with DOI was larger than that of saline-injected rats (DOI injected at P21 and recorded at P23) (Figure 4B), indicating synaptic delivery of endogenous AMPARs in non-VD rats injected with DOI. To exclude the possibility that DOI injection in the barrel cortex would influence whisking behavior, we next compared synaptic GluR1 delivery under the same whisker-input in the presence and absence of DOI. We microinjected Herpes simplex virus expressing GFP-GluR1 into layer 2/3 of the barrel cortex together with DOI or vehicle at P21. One day later, we anesthetized infected animals and stimulated whiskers mechanically for 6 hr (Figure 4C; see Experimental Procedures). We then prepared acute brain slices and recorded transmission of layer 4-2/3 synapses. An increase in rectification values could only be detected in GFP-GluR1 expressing pyramidal neurons that were exposed to DOI (Figure 4D). These findings suggest that increased levels of extracellular serotonin in the barrel cortex is sufficient to facilitate synaptic plasticity through activation of 5HT2A/2C receptors, promoting whisker experience-dependent delivery of GluR1 in animals subjected to VD.

To further investigate whether serotonin signaling facilitates synaptic delivery of endogenous GluR1-containing receptors, we examined the effect of increased 5HT2A/2C agonist levels on synaptic plasticity. We prepared acute brain slices from intact animals aged P23 and induced synaptic plasticity at layer 4-2/3 synapses of the rat barrel cortex in the absence or presence of DOI. We paired 1 Hz stimulation (3 min) with postsynaptic potential at −40 mV. While this protocol exhibited no effect on synaptic responses in the absence of DOI, it elicited LTP in the presence of DOI (Figure 4E). When we paired 1 Hz stimulation with post-synaptic potential at 0 mV, LTP was induced in animals both in the presence and absence of DOI (Figure 4F). We also found that DOI facilitates LTP induction by a different LTP-inducing protocol (theta burst stimulation, see Experimental Procedures for the induction protocol; with DOI: 136% ± 3.0%, n = 4, without DOI: 96.1% ± 6.0%, n = 5, $p < 0.05$, Student's t test. Mean amplitude between 30 and 40 min after induction was normalized to base line amplitude) (Figure S4). These experiments show that serotonin acts via activation of 5HT2A/2C receptors to facilitate GluR1 delivery and concurrently lowering the threshold for LTP.

VD Induces Phosphorylation of GluR1 at a Site Critical for Its Synaptic Delivery

The GluR1 subunit can be phosphorylated by PKA at Ser845, and this phosphorylation event has previously been shown to lower the threshold for LTP induction (Esteban et al., 2003; Hu et al., 2007; Song and Huganir, 2002). To examine whether VD-mediated facilitation of synaptic strengthening involves phosphorylation of GluR1 at Ser845, we isolated crude lysate preparations from the barrel cortex of either VD (P21–P23) or nondeprived animals at P23 and measured the levels of Ser845 phosphorylated GluR1 relative to total GluR1 amounts. VD led to an increase in the proportion of GluR1 that is phosphorylated at Ser845 (Figure 5A). The VD-induced increase in phosphorylation of Ser845 was prevented by the local injection of ketanserin in the barrel cortex (Figure 5B), indicating that VD-induced phosphorylation of Ser845 is mediated by serotonin signaling.

ERK activation regulates synaptic insertion of GluR1 by triggering phosphorylation of Ser845 of GluR1 (Qin et al., 2005). Since serotonin activates ERK through 5HT2A receptors in neuronal cells (Johnson-Farley et al., 2005; Quinn et al., 2002), we tested if VD activates ERK (p42) in the barrel cortex. Crude lysate prepared at P23 exhibited increased phosphorylation of ERK in VD animals (P21–P23) compared with control animals (Figure 5C), indicating that VD induced ERK activation in the barrel cortex. As was the case with the phosphorylation at Ser845, the increase of ERK activation by VD was diminished by the local injection of 5HT2A/2C receptor antagonist ketanserin (Figure 5D). These results suggest that VD increases GluR1 phosphorylation at Ser845 by serotonin-mediated activation of ERK.

To test if the increase of GluR1 phosphorylation at Ser845 in VD animals is crucial for VD-induced synaptic GluR1 delivery, we introduced a GluR1 construct with serine845 mutated to alanine (S845A) in the barrel cortex of VD animals (VD during P21–P23) at P21 by viral-mediated in vivo gene transfer. We failed to detect an increase in rectification in GluR1 S845A expressing neurons compared to nearby uninfected neurons (Figure S5). These data suggest that GluR1 phosphorylation at Ser845 plays a critical role in the synaptic strengthening in barrel cortex of animals that underwent VD.

VD Sharpened Functional Whisker-Barrel Map at Layer 2/3 in the Barrel Cortex

The increase in serotonin release in the barrel cortex led to a selective strengthening of layer 2/3 synapses that receive input from within a cortical column, but not of synapses that are innervated by lateral input from neighboring columns (Figure 1E). We wondered whether the VD-induced synaptic plasticity in the barrel cortex would improve the accuracy of

whisker function. VD-driven GluR1 delivery into layer 4-2/3 synapses of the barrel cortex could sharpen the functional relationship between whisker and barrel column at layer 2/3. To test this possibility, we examined receptive fields of layer 2/3 of the barrel cortex in the absence or presence of VD. Two days after VD, single-unit in vivo recordings were performed in anaesthetized rats to assess the functional whisker-barrel map. We measured the number of spikes evoked in response to deflections of multiple single whiskers. Whiskers that exhibited the largest response were defined as principal whiskers. We found that the relative response of surrounding whiskers to the response evoked by stimulation of the principal whiskers was lower in rats exposed to VD than in control rats, indicating that functional receptive fields of layer 2/3 in the barrel cortex were sharpened by VD (Figure 6A). This effect by VD is serotonin-signaling dependent, since local injection of ketanserin during VD prevented sharpening of the functional whisker-barrel map (Figure 6B).

To examine whether the sharpened functional whisker-barrel map in VD animals were due to synaptic delivery of GluR1, we expressed the plasticity-blocker GFP-GluR1ct in the barrel cortex by means of viral-mediated gene transfer. We injected Herpes simplex virus expressing either GFP-GluR1ct or GFP in the layer 2/3 of the barrel cortex at P21. We sutured both eyes immediately after viral infection and examined the functional whisker barrel map in layer 2/3 by in vivo recording at age P23. The relative response evoked in surrounding whiskers to the response at principal whiskers was higher in rats expressing GFP-GluR1ct than in control rats expressing GFP alone (Figure 6C). Thus, the VD induced improvement in the functional whisker-barrel map was prevented by expression of GFP-GluR1ct. These experiments demonstrate that the sharpening of the functional whisker-barrel map observed in rats exposed to VD depends on serotonin-mediated synaptic GluR1 delivery.

DISCUSSION

While the occurrence of cross-modal plasticity (i.e., the cortical reorganization to compensate for the loss of one sensory system with other intact modalities) is well documented, our knowledge about the neuronal mechanisms underlying this form of plasticity has been limited (Bavelier and Neville, 2002; Goel et al., 2006). In this study, we focused on cross-modal changes between visual and somatosensory systems that rodents utilize to acquire spatial information. We here provide a comprehensive description of the molecular, synaptic, and circuit mechanisms underlying cross-modal reorganization of cortices. We here demonstrate that loss of vision leads to a significantly increased release of serotonin in the barrel cortex, but not in the visual cortex. These increased serotonin levels are sufficient and necessary to cause synaptic plasticity in excitatory barrel neurons, leading to fine-tuning of the whisker-barrel map.

Although evidence of the enhancement of neural plasticity with the activation of serotonergic system has been well established (Bennett-Clarke et al., 1994, 1995; Chen et al., 2003; Inaba et al., 2009; Jones et al., 2009; Kim et al., 2006; Kojic et al., 1997; Maya Vetencourt et al., 2008; Normann and Clark, 2005; Turlejski et al., 1997), the molecular basis underlying it remained elusive. Furthermore, the physiological roles of the effects of serotonergic system on synaptic plasticity in vivo are not well characterized. Our study provides evidence that the activation of serotonergic system increases synaptic plasticity through the facilitation of AMPARs delivery into synapses during cross-modal cortical reorganization. In addition, we elucidate the signaling mechanisms of how the activation of serotonergic system facilitates synaptic GluR1 delivery. We found that knock down of postsynaptic 5HT2A receptors prevents AMPARs delivery into layer 4-2/3 synapses of the barrel cortex of VD rats. Our data suggest that VD-driven serotonin release acts directly at neurons at the postsynaptic site by modulating intracellular signaling pathways required for

AMPARs delivery. We showed that VD increased GluR1 phosphorylation at Ser845, a critical site for synaptic AMPARs delivery. Furthermore, we found that ERK, a downstream signaling molecule of 5HT2A/C receptors (Johnson-Farley et al., 2005; Quinn et al., 2002; Raymond et al., 2001), was activated by VD in a serotonin-mediated fashion. ERK activation leads to GluR1 phosphorylation at Ser845 (Qin et al., 2005). Taken together, our results suggest that VD stimulates the serotonergic system in the barrel cortex, leading to ERK activation through 5HT2A/2C receptors, and increases in GluR1 phosphorylation at Ser845. Phosphorylation of GluR1 at Ser845 has been demonstrated to enhance surface expression of GluR1 (Derkach et al., 2007), and synaptic insertion of GluR1 is mostly mediated by lateral diffusion from extra-synaptic sites (Makino and Malinow, 2009). Thus, VD may facilitate synaptic GluR1 delivery by increasing the extrasynaptic pool of GluR1 through phosphorylating GluR1. Consistent with this hypothesis, we detected no increased synaptic GluR1 delivery in VD animals when a mutant GluR1 was expressed in which S845 phosphorylation was blocked (Figure S5). Although increases in extracellular serotonin in the barrel cortex may lower the threshold for synaptic GluR1 delivery in a large number of layer 2/3 synapses within the barrel cortex, we observed that synaptic potentiation mainly occurred at layer 2/3 synapses that receive input from layer 4. A potential explanation for this selective effect of increased serotonin-signaling is that only those synapses that receive robust inputs from presynaptic neurons will be strengthened, while synapses that receive little input will remain unchanged.

Although we found that reducing the expression levels of 5HT2A receptors postsynaptically in layer2/3 neurons was sufficient to block VD-driven synaptic strengthening, it is possible that presynaptic sites or other types of serotonin receptors also contribute to VD-driven synaptic enhancement at layer4-2/3 synapses in the barrel cortex. Since 5HT2A and 5HT2C receptors share a similar downstream signaling cascades, both receptors could mediate VD-induced facilitation of synaptic AMPARs delivery at the postsynaptic site. Alternatively, presynaptic 5HT2C receptors could contribute to VD-driven synaptic enhancement at layer4-2/3 synapses in the barrel cortex, because high expression of 5HT2C receptors was detected in the layer 4 of the barrel cortex at the experimental age (Li et al., 2004). Further study will be required to discriminate these possibilities.

The VD-driven GluR1 delivery in layer 2/3 neurons of the barrel cortex appears to be confined to synapses that receive input from layer 4, since VD did not elicit synaptic GluR1 delivery at the lateral pathway (Figure 1E). This leads to specific strengthening of the neuronal connectivity responsible for the response to the principal whisker (layer 4-2/3 synapses within a cortical column) but not that for the response to the surrounding whiskers (e.g., intracortical pathway). This should cause an enhancement of the response to the principal whisker relative to the response to surrounding whiskers and result in the sharpening of the functional whisker-barrel map. While we found that 2 days of VD saturated AMPARs contents and occluded LTP at layer 4-2/3 synapses (Figure 2), LTP can be induced at other synapses from layer 4 even after 2 days of VD.

We here demonstrate that within 2 days after VD synapses were strengthened selectively at layer 4-2/3 synapses in the barrel cortex, leading to sharpening of whisker-barrel function. A previous study reported that after 7 days of loss of visual experience the amplitudes of AMPARs-mediated miniature EPSCs (mEPSC) at layer 2/3 of the barrel cortex and rectification at layer 4-2/3 synapses of the barrel cortex were reduced (Goel et al., 2006). It is possible that an initial selective strengthening of synapses during the acute phase of VD is followed by gradual decrease in average synaptic transmission 1 week after the start of VD due to a homeostatic plasticity mechanism. Indeed, we confirmed that 7 days of VD decreased A/N ratio and rectification at layer 4-2/3 synapses of the barrel cortex (Figures S1A and S1B). Although synaptic transmission was decreased 1 week after the beginning of

VD, sharpened whisker-barrel function can still be maintained. The relative synaptic strengthening of the vertical pathway to the horizontal pathway, which was initially established during the acute phase of VD, can be maintained despite a gradual overall reduction in synaptic transmission in a later phase. A sustained enhancement of lateral inhibition might be established by the acute synaptic strengthening at vertical pathway (layer 4-2/3 synapses). It will be interesting to test if VD induces persistent improvement of whisker functions.

Animals that are visually deprived will depend more on their whiskers to navigate through their external environment. In other words, when blind, their attention needs to be directed more toward receiving somatosensory input than when vision is intact. Serotonergic neurons from dorsal raphe nucleus innervate various brain areas and have been suggested to control the coordinated reorganization among different cortical regions driven by higher order cognitive functions such as attention (Geyer and Vollenweider, 2008; Vertes, 1991). Interestingly, we found that the number of neurons that were activated (i.e., expressing c-Fos) within the area of dorsal raphe nucleus that innervates barrel cortex was significantly higher in VD animals compared with intact animals (Figures S3D–S3G). Furthermore, we detected no significant increase of c-Fos positive neurons in the area of dorsal raphe nucleus which innervates visual cortex in VD rats (data not shown), indicating selective activation of serotonergic neurons that innervate barrel cortex in animals with VD. It will be interesting to learn the neural circuit regulating such a selective activation of serotonergic neurons.

In conclusion, we here show that cross-modal plasticity depends on synaptic AMPARs trafficking and is mediated through selective serotonin signaling at brain areas that need to compensate for the loss of function in the input-deprived brain area. Understanding the molecular mechanism through which cross-modal plasticity is established may further our knowledge of how to selectively restore or retune neuronal circuits in patients that suffered from sensory dysfunction.

EXPERIMENTAL PROCEDURES

Animals

Since large number of studies utilized Long-Evans rats to investigate visual function, we used this strain for this study. Male juvenile Long-Evans rats (postnatal day 21–25) were housed on a 12-hr-light/dark cycle with ad libitum access to water and food. Procedures were performed in strict compliance with the animal use and care guidelines of Yokohama City University.

Electrophysiology

Thirty-six hours after virus injection, rats were anesthetized with isoflurene gas and brains were removed. Brains were quickly transferred into ice-cold dissection buffer (25.0 mM $NaHCO_3$, 1.25 mM NaH_2PO_4, 2.5 mM KCl, 0.5 mM $CaCl_2$, 7.0 mM $MgCl_2$, 25.0 mM glucose, 110.0 mM choline chloride, 11.6 mM ascorbic acid, 3.1 mM pyruvic acid) gassed with 5% CO_2/95%O_2. Coronal brain slices were cut (300 μm, Leica vibratome) in dissection buffer and transferred to physiological solution (22°C–25°C, 118 mM NaCl, 2.5 mM KCl, 26.2 mM NaHCO3, 1 mM NaH2PO4, 11 mM glucose, 1.3 mM $MgCl_2$, 2.5 mM $CaCl_2$ [pH 7.4] gassed with 5% CO_2/95%O_2). The recording chamber was perfused with physiological solution containing 0.1 mM picrotoxin, 4 μM 2-chloroadenosine at 22°C–25°C. For rectification experiments, we added 0.1 mM D,L-APV to perfusate to block NMDARs. Patch recording pipettes (3–7 MΩ) were filled with intracellular solution (115 mM cesium methanesulfonate, 20 mM CsCl, 10 mM HEPES, 2.5 mM $MgCl_2$, 4 mM Na_2ATP, 0.4 mM Na_3GTP, 10 mM sodium phosphocreatine, 0.6 mM EGTA [pH 7.25]). Whole-cell

recordings were obtained from infected or uninfected layer 2/3 pyramidal neurons (150–500 μm from pial surface) of the rat barrel cortex with Multiclamp 700B (Axon Instruments). There were no significant differences in input or series resistance among groups (infected, noninfected, intact, deprived). Bipolar tungsten stimulating electrodes were placed in layer 4 ~200–300 μm below recorded cells. Stimulus intensity was increased until a synaptic response of amplitude > ~10 pA was recorded. When recording simultaneously from two cells, stimulus intensity was increased until a) both cells showed response > ~10 pA, or b) one cell showed response > ~10 pA and a stronger stimulus produced epileptiform bursting. Synaptic AMPA-R mediated responses at −60 mV and +40 mV were averaged over 50–100 trials and their ratio was used as an index of rectification (Hayashi et al., 2000). AMPA/NMDA ratios were calculated as the ratio of peak current at −60 mV to the current at +40 mV 50 ms after stimulus onset (40–50 traces averaged for each holding potential).

In experiments analyzing long-term potentiation in slices from visually deprived or intact rats were maintained in ACSF. In a subset of experiments standard ACSF was used as described above. In order to monitor synaptic transmission we evoked AMPA postsynaptic currents at two synaptic pathways by interleaved stimulation of two fiber bundles at 0.33–0.1 Hz and recorded at −60 mV holding potential in voltage-clamp mode. LTP was induced at one pathway by a pairing protocol consisting of presynaptic fiber stimulation at 5 Hz for 90 s paired with postsynaptic depolarization to 20 mV holding potential in occlusion experiments. For experiments to examine the effect of DOI on LTP, we paired 1 Hz stimulation (3 min) with postsynaptic potential either at −40 or 0 mV. For theta burst stimulation (TBS), layer 4-2/3 synapses were stimulated with 5 Hz trains of 5 theta bursts containing five pulses at 100 Hz (bursts were separated by 200 ms). The postsynaptic potential was held at −40 mV, when TBS was applied and switched back to −60 mV afterward. Experiments were excluded from analysis if unpaired control pathways displayed changes in transmission.

For the recording of the asynchronous quantal AMPAR-EPSCs (Sr^{2+}-mEPSCs), $CaCl_2$ was replaced with 2 mM $SrCl_2$, and 2-chloroadenosine was removed. Sr^{2+}-mEPSCs were detected and analyzed using Clampfit10.2 software (Axon Instruments). The detection threshold for Sr^{2+}-mEPSCs was set at 10 pA (2× RMS noise). Asynchronous synaptic events were picked up from events that occurred between 200 and 900 ms after the stimulation. (See Supplemental Information for details.)

Infection of Neocortical Neurons In Vivo

At PND21, rats were anesthetized with a ketamine/xylazine cocktail (ketamine: 0.56 mg/g body weight; xylazine: 0.03 mg/g body weight). The skin overlying the skull was cut and gently pushed to the side. The anterior fontanel was identified and a region 2 mm posterior, 5 mm lateral was gently pierced with a dental drill. Coordinates were independently ascertained to correspond to the barrel cortex by cytochrome oxidase staining. Glass pipettes (tip diameter ~12 μm) were used to inject recombinant Herpes virus into the barrel cortex. After injection, the skin was repositioned and maintained with cyanoacrylate glue. During procedures, animals were kept on a heating pad and were brought back into their home cages after regaining movement. Visual deprivation was initiated by suturing eyelids immediately after injection of virus. (See Supplemental Experimental Procedures for details.)

Drug Treatment

DOI (2,5-dimethoxy-4-iodoamphetamine), a specific agonist of 5HT2A/2C receptors, ketanserin, or an antagonist of 5HT2A/2C was simultaneously injected with GFP-GluR1

expressing Herpes virus into the barrel cortex at P21 (DOI: 2 mM, ketanserin: 1 mM). For LTP experiment, DOI (final 20 μM) was bath applied.

In Vivo Microdialysis

Visually deprived or intact rats were anesthetized and stereotaxically implanted with stainless-steel guide cannula (outer diameter, 0.51 mm; AG-4, Eicom Co., Kyoto, Japan) into the barrel cortex. The coordinates were 2 mm anterior from the bregma, 4.5 mm lateral to the midline, and 0.2 mm below the surface of the brain. After cannula implantation, a stylet was inserted into the guide until the microdialysis experiment. (See Supplemental Experimental Procedures for details.)

5HT Assay

5HT concentration in the dialysate was quantified by high performance liquid chromatography with a pump system (EP-300; Eicom Co.). (See Supplemental Experimental Procedures for details.)

In Vivo Recording

At P23, rats were anesthetized with urethane (31.25 mg/kg, body weight). The skull on the barrel cortex was exposed as described above. Concentric bipolar electrodes (Rhodes Medical) were inserted 200–400 μm below the pia. Single whiskers on the contralateral side were stimulated using a metal needle mounted on a piezoelectric wafer. For each stimulus trial, a whisker was moved up followed by a downward deflection after 1 s. The movement was 0.5 mm at 1 mm away from the skin. Spikes in response to whisker stimulus were recorded with Powerlab 4/25 (AD instruments). The number of spikes recorded 5–50 ms after whisker deflection was counted and used as a measure of the response. Whiskers that exhibited the largest response were defined as principal whiskers. Electrode positions were marked by over-current injection and analyzed histologically after each experiment.

Biochemical Analysis

Barrel cortex samples were rapidly dissected out and stored at −80°C until assayed. Frozen samples were ice-cold homogenation buffer using glass-glass tissue homogenizer. Homogenates were sonicated in 1% SDS and boiled for 10 min. (See Supplemental Experimental Procedures for details.)

Immunohistochemistry

VD or intact animals were anesthetized with an overdose of sodium pentobarbital, and then perfused transcardially with heparinized saline followed by 4% paraformaldehyde in 0.1 M phosphate buffer (pH 7.4). Coronal sections of the midbrain (30 μm) were prepared with a cryostat. Sections were incubated overnight at room temperature in a PBS solution containing anti c-Fos polyclonal antibody (1:40,000, Calbiochem). (See Supplemental Experimental Procedures for details.)

Artificial Stimulation of Rat Whiskers

At PND21, rats were injected with recombinant Herpes virus expressing GFP-GluR1 into the barrel cortex. Twenty-four hours after injection, rats were anesthetized with urethane (25 mg/body weight) and injected with DOI or saline into the barrel cortex as same coordination of virus injection. After injection, whiskers of rats were stimulated by rotating a needle set to motor device (Mabuchi motor RE-240RA-2670: 6300 rpm) for 5–6 hr. Animals were kept on a heating pad during procedures. After stimulation, rats were decapitated and brain slices were prepared for the electrophysiological assay.

Supplementary Material

Refer to Web version on PubMed Central for supplementary material.

Acknowledgments

This project was supported by JST, CREST (T.T.), Special Coordination Funds for Promoting Science and Technology (T.T.), “Development of biomarker candidates for social behavior” carried out under the Strategic Research Program for Brain Sciences by the Ministry of Education, Culture, Sports,-Science and Technology of Japan (TT), and Ishidsu Shun Memorial Scholarship (S.J.). We thank Dr. Philippe Marin (Institute de génomique fonctionnelle) for supporting the short hairpin constructs and characterization in his laboratory. We thank Yoshiko Kanno and Yoshinori Kamiya for technical assistance. We thank Dr. Hiroyuki Miyoshi and Atsushi Miyawaki (RIKEN) for providing Lenti-virus vector. We thank Kenkichi Takase Himeji Dokkyo) for discussion. We also thank Yasunori Hayashi (RIKEN) and Jose Esteban (CSIC) for critically reading the manuscript.

References

Barry MF, Ziff EB. Receptor trafficking and the plasticity of excitatory synapses. Curr Opin Neurobiol. 2002; 12:279–286. [PubMed: 12049934]

Bavelier D, Neville HJ. Cross-modal plasticity: Where and how? Nat Rev Neurosci. 2002; 3:443–452. [PubMed: 12042879]

Bennett-Clarke CA, Leslie MJ, Lane RD, Rhoades RW. Effect of serotonin depletion on vibrissa-related patterns of thalamic afferents in the rat’s somatosensory cortex. J Neurosci. 1994; 14:7594–7607. [PubMed: 7996198]

Bennett-Clarke CA, Lane RD, Rhoades RW. Fenfluramine depletes serotonin from the developing cortex and alters thalamocortical organization. Brain Res. 1995; 702:255–260. [PubMed: 8846085]

Bredt DS, Nicoll RA. AMPA receptor trafficking at excitatory synapses. Neuron. 2003; 40:361–379. [PubMed: 14556714]

Chen A, Hough CJ, Li H. Serotonin type II receptor activation facilitates synaptic plasticity via N-methyl-D-aspartate-mediated mechanism in the rat basolateral amygdala. Neuroscience. 2003; 119:53–63. [PubMed: 12763068]

Clark RE, Squire LR. Classical conditioning and brain systems: The role of awareness. Science. 1998; 280:77–81. [PubMed: 9525860]

Clem RL, Barth A. Pathway-specific trafficking of native AMPARs by in vivo experience. Neuron. 2006; 49:663–670. [PubMed: 16504942]

Derkach VA, Oh MC, Guire ES, Soderling TR. Regulatory mechanisms of AMPA receptors in synaptic plasticity. Nat Rev Neurosci. 2007; 8:101–113. [PubMed: 17237803]

Diamond ME, Huang W, Ebner FF. Laminar comparison of somatosensory cortical plasticity. Science. 1994; 265:1885–1888. [PubMed: 8091215]

Dye MW, Baril DE, Bavelier D. Which aspects of visual attention are changed by deafness? The case of the Attentional Network. Test Neuropsychologia. 2007; 45:1801–1811.

Esteban JA, Shi SH, Wilson C, Nuriya M, Huganir RL, Malinow R. PKA phosphorylation of AMPA receptor subunits controls synaptic trafficking underlying plasticity. Nat Neurosci. 2003; 6:136–143. [PubMed: 12536214]

Geyer MA, Vollenweider FX. Serotonin research: Contributions to understanding psychoses. Trends Pharmacol Sci. 2008; 29:445–453. [PubMed: 19086254]

Goel A, Jiang B, Xu LW, Song L, Kirkwood A, Lee HK. Cross-modal regulation of synaptic AMPA receptors in primary sensory cortices by visual experience. Nat Neurosci. 2006; 9:1001–1003. [PubMed: 16819524]

Hayashi Y, Shi SH, Esteban JA, Piccini A, Poncer JC, Malinow R. Driving AMPA receptors into synapses by LTP and CaMKII: Requirement for GluR1 and PDZ domain interaction. Science. 2000; 287:2262–2267. [PubMed: 10731148]

Hollmann M, Heinemann S. Cloned glutamate receptors. Annu Rev Neurosci. 1994; 17:31–108. [PubMed: 8210177]

Holtmaat A, Svoboda K. Experience-dependent structural synaptic plasticity in the mammalian brain. Nat Rev Neurosci. 2009; 10:647–658. [PubMed: 19693029]

Hu H, Real E, Takamiya K, Kang MG, Ledoux J, Huganir RL, Malinow R. Emotion enhances learning via norepinephrine regulation of AMPA-receptor trafficking. Cell. 2007; 131:160–173. [PubMed: 17923095]

Inaba M, Maruyama T, Yoshimura Y, Hosoi H, Komatsu Y. Facilitation of low-frequency stimulation-induced long-term potentiation by endogenous noradrenaline and serotonin in developing rat visual cortex. Neurosci Res. 2009; 64:191–198. [PubMed: 19428700]

Johnson-Farley NN, Kertesy SB, Dubyak GR, Cowen DS. Enhanced activation of Akt and extracellular-regulated kinase pathways by simultaneous occupancy of Gq-coupled 5-HT2A receptors and Gs-coupled 5-HT7A receptors in PC12 cells. J Neurochem. 2005; 92:72–82. [PubMed: 15606897]

Jones KA, Srivastava DP, Allen JA, Strachan RT, Roth BL, Penzes P. Rapid modulation of spine morphology by the 5-HT2A serotonin receptor through kalirin-7 signaling. Proc Natl Acad Sci USA. 2009; 106:19575–19580. [PubMed: 19889983]

Kessels HW, Malinow R. Synaptic AMPA receptor plasticity and behavior. Neuron. 2009; 61:340–350. [PubMed: 19217372]

Kim HS, Jang HJ, Cho KH, Hahn SJ, Kim MJ, Yoon SH, Jo YH, Kim MS, Rhie DJ. Serotonin inhibits the induction of NMDA receptor-dependent long-term potentiation in the rat primary visual cortex. Brain Res. 2006; 1103:49–55. [PubMed: 16784733]

Kojic L, Gu Q, Douglas RM, Cynader MS. Serotonin facilitates synaptic plasticity in kitten visual cortex: An in vitro study. Brain Res Dev Brain Res. 1997; 101:299–304.

Li QH, Nakadate K, Tanaka-Nakadate S, Nakatsuka D, Cui Y, Watanabe Y. Unique expression patterns of 5-HT2A and 5-HT2C receptors in the rat brain during postnatal development: Western blot and immunohistochemical analyses. J Comp Neurol. 2004; 469:128–140. [PubMed: 14689478]

Macaluso E, Driver J. Spatial attention and crossmodal interactions between vision and touch. Neuropsychologia. 2001; 39:1304–1316. [PubMed: 11566313]

Makino H, Malinow R. AMPA receptor incorporation into synapses during LTP: The role of lateral movement and exocytosis. Neuron. 2009; 64:381–390. [PubMed: 19914186]

Malinow R, Malenka RC. AMPA receptor trafficking and synaptic plasticity. Annu Rev Neurosci. 2002; 25:103–126. [PubMed: 12052905]

Mansour M, Nagarajan N, Nehring RB, Clements JD, Rosenmund C. Heteromeric AMPA receptors assemble with a preferred subunit stoichiometry and spatial arrangement. Neuron. 2001; 32:841–853. [PubMed: 11738030]

Maya Vetencourt JF, Sale A, Viegi A, Baroncelli L, De Pasquale R, O'Leary OF, Castren E, Maffei L. The antidepressant fluoxetine restores plasticity in the adult visual cortex. Science. 2008; 320:385–388. [PubMed: 18420937]

McIntosh AR, Rajah MN, Lobaugh NJ. Interactions of prefrontal cortex in relation to awareness in sensory learning. Science. 1999; 284:1531–1533. [PubMed: 10348741]

Normann C, Clark K. Selective modulation of Ca(2+) influx pathways by 5-HT regulates synaptic long-term plasticity in the hippocampus. Brain Res. 2005; 1037:187–193. [PubMed: 15777768]

Qin Y, Zhu Y, Baumgart JP, Stornetta RL, Seidenman K, Mack V, van Aelst L, Zhu JJ. State-dependent Ras signaling and AMPA receptor trafficking. Genes Dev. 2005; 19:2000–2015. [PubMed: 16107614]

Quinn JC, Johnson-Farley NN, Yoon J, Cowen DS. Activation of extracellular-regulated kinase by 5-hydroxytryptamine(2A) receptors in PC12 cells is protein kinase C-independent and requires calmodulin and tyrosine kinases. J Pharmacol Exp Ther. 2002; 303:746–752. [PubMed: 12388661]

Rauschecker JP, Tian B, Korte M, Egert U. Crossmodal changes in the somatosensory vibrissa/barrel system of visually deprived animals. Proc Natl Acad Sci USA. 1992; 89:5063–5067. [PubMed: 1594614]

Raymond JR, Mukhin YV, Gelasco A, Turner J, Collinsworth G, Gettys TW, Grewal JS, Garnovskaya MN. Multiplicity of mechanisms of serotonin receptor signal transduction. Pharmacol Ther. 2001; 92:179–212. [PubMed: 11916537]

Rumpel S, LeDoux J, Zador A, Malinow R. Postsynaptic receptor trafficking underlying a form of associative learning. Science. 2005; 308:83–88. [PubMed: 15746389]

Sadato N, Pascual-Leone A, Grafman J, Ibanez V, Deiber MP, Dold G, Hallett M. Activation of the primary visual cortex by Braille reading in blind subjects. Nature. 1996; 380:526–528. [PubMed: 8606771]

Scannevin RH, Huganir RL. Postsynaptic organization and regulation of excitatory synapses. Nat Rev Neurosci. 2000; 1:133–141. [PubMed: 11252776]

Shi S, Hayashi Y, Esteban JA, Malinow R. Subunit-specific rules governing AMPA receptor trafficking to synapses in hippocampal pyramidal neurons. Cell. 2001; 105:331–343. [PubMed: 11348590]

Shi SH, Hayashi Y, Petralia RS, Zaman SH, Wenthold RJ, Svoboda K, Malinow R. Rapid spine delivery and redistribution of AMPA receptors after synaptic NMDA receptor activation. Science. 1999; 284:1811–1816. [PubMed: 10364548]

Song I, Huganir RL. Regulation of AMPA receptors during synaptic plasticity. Trends Neurosci. 2002; 25:578–588. [PubMed: 12392933]

Stern EA, Maravall M, Svoboda K. Rapid development and plasticity of layer 2/3 maps in rat barrel cortex in vivo. Neuron. 2001; 31:305–315. [PubMed: 11502260]

Takahashi T, Svoboda K, Malinow R. Experience strengthening transmission by driving AMPA receptors into synapses. Science. 2003; 299:1585–1588. [PubMed: 12624270]

Turlejski K, Djavadian RL, Kossut M. Neonatal serotonin depletion modifies development but not plasticity in rat barrel cortex. Neuroreport. 1997; 8:1823–1828. [PubMed: 9223059]

Vertes RP. A PHA-L analysis of ascending projections of the dorsal raphe nucleus in the rat. J Comp Neurol. 1991; 313:643–668. [PubMed: 1783685]

Wenthold RJ, Petralia RS, Blahos J II, Niedzielski AS. Evidence for multiple AMPA receptor complexes in hippocampal CA1/CA2 neurons. J Neurosci. 1996; 16:1982–1989. [PubMed: 8604042]

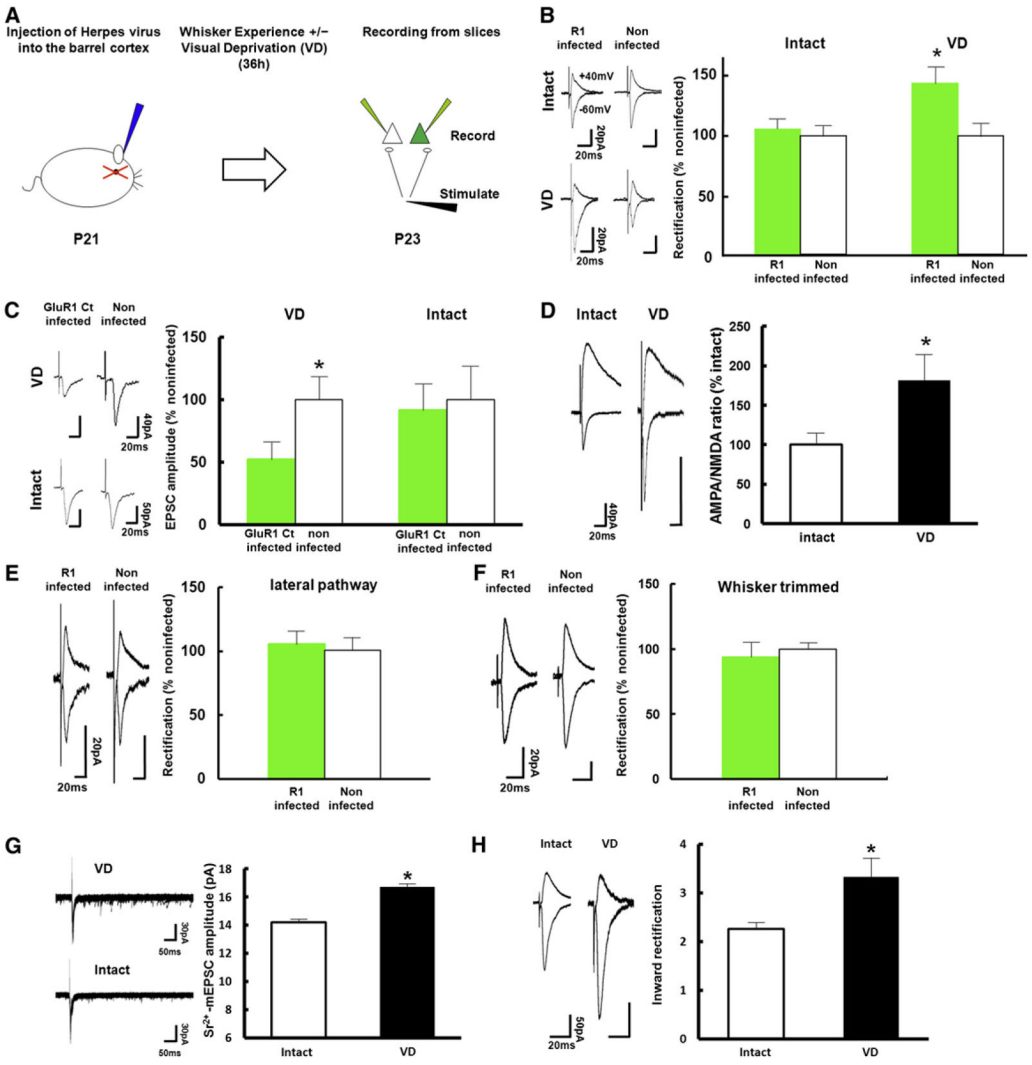

Figure 1. VD Drives GluR1 into Layer 4 to Layer 2/3 Synapses of the Barrel Cortex in Juvenile Rats

(A) Experimental protocol (see text for details).

(B) (Left) Synaptic responses (average of 50 consecutive trials) from infected with GFP-GluR1 expressing virus and noninfected neurons (held at −60 and +40 mV, as indicated) of juvenile rats (P21–P23) with intact or sutured eyes (VD). (Right) Graph of average rectification indices (RI: response at −60 mV/response at +40 mV) of neurons expressing GFP-GluR1 (green), normalized to RI value of nearby noninfected cells (white). Intact: n = 14, VD: n = 10. Scale bars are as indicated. *Statistical difference ($p < 0.05$. Student's t test). Error bars indicate ± SEM.

(C) (Left) Synaptic responses from layer 4 to layer 2/3 pyramidal neurons infected with GFP-GluR1ct (labeled as GluR1 ct infected) expressing virus or noninfected in the barrel cortex of rats with or without VD were recorded by simultaneous whole-cell recordings. (Right) Graph of mean AMPARs-mediated transmission onto infected neurons (green), normalized to values obtained in noninfected neurons (white). Note synaptic depression of GFP-GluR1ct expressing neurons compared with nonexpressing neurons of animals with VD, while no difference in synaptic transmission was detected with intact animals. Intact: n

= 9, VD: n = 10. Scale bars are as indicated. *Statistical difference ($p < 0.05$, Wilcoxon nonparametric test). Error bars indicate ± SEM.

(D) (Left) Synaptic responses from layer 4 to layer 2/3 pyramidal neurons in the barrel cortex of rats with intact or sutured eyes (VD). (Right) Graph of mean ratio of AMPARs-mediated currents to NMDA receptor-mediated currents (A/N ratio) of VD rats normalized to that of intact rats. Note that A/N ratio of VD rats (black) was larger than that of intact rats (white), suggesting that VD drives endogenous AMPARs into synapses. Intact: n = 17, VD: n = 13. Scale bars are as indicated. *Statistical difference ($p < 0.05$, Student's t test). Error bars indicate ± SEM.

(E) (Left) Synaptic responses from layer 2/3 to layer 2/3 pyramidal neurons (lateral pathway) infected with GFP-GluR1 expressing virus and noninfected neurons of juvenile VD rats (P21–P23). Note no difference of rectification between infected and noninfected neurons. (Right) Graph of average RI of neurons expressing GFP-GluR1 (green), normalized to RI value of nearby noninfected cells (white). n = 7. Scale bars are as indicated. Note that there was no statistical difference. Error bars indicate ± SEM.

(F) (Left) Synaptic responses from layer 4 to layer 2/3 pyramidal neurons infected with GFP-GluR1 expressing virus and noninfected neurons of juvenile VD rats with whiskers trimmed (P21–P23). Note no difference of rectification between infected and noninfected neurons. (Right) Graph of average RI of neurons expressing GFP-GluR1 (green), normalized to RI value of nearby noninfected cells (white). n = 6. Scale bars are as indicated. Note that there was no statistical difference. Error bars indicate ± SEM.

(G) (Left) Evoked quantal EPSC responses at layer 4 to layer 2/3 synapses in the barrel cortex of VD and intact animals. (Right) The average amplitude of evoked quantal EPSC. Note that evoked quantal EPSC of VD animals was larger than intact animals. Intact animals: n = 191 events. VD animals: n = 294 events. Scale bars are as indicated. *Statistical difference ($p < 0.001$, Kolmogorov-Smirnov test). Error bars indicate ± SEM.

(H) (Left) Synaptic responses from layer 4 to layer 2/3 pyramidal neurons in the barrel cortex of rats with intact or sutured eyes (VD for 2 days). (Right) Graph of average RI of neurons from intact and VD animals. Intact animals: n = 12, VD: n = 10. Scale bars are as indicated. *Statistical difference ($p < 0.05$, Student's t test).
Error bars indicate ± SEM.

See also Figure S1.

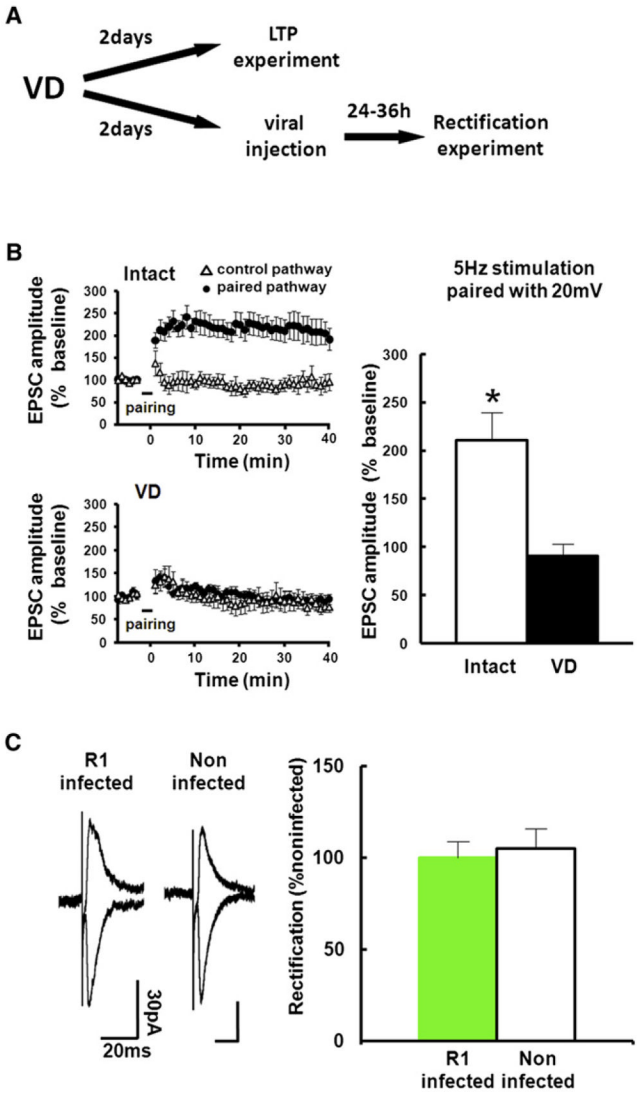

Figure 2. VD Procedure for 2 Days Occludes LTP in the Barrel Cortex

(A) Experimental protocol. We sutured both eyes at P21. For LTP experiment, acute brain slices were prepared at P23. Then LTP at layer 4-2/3 synapses of the barrel cortex was induced by pairing postsynaptic depolarization (+20 mV) with presynaptic stimulation (5 Hz, 90 s). For the rectification experiment, we microinjected GFP-GluR1 expressing virus at P23, and whole-cell recordings were performed at P25.

(B) Recordings were maintained for at least 40 min after pairing. (Left) The EPSC amplitude was normalized to the average baseline amplitude before pairing. Paired pathways (black circle) and control pathways (triangle) of intact and VD animals are shown. (Right) Mean amplitude between 30 and 40 min after induction was normalized to base line amplitude. While LTP was successfully induced in intact rats, LTP induction was prevented in animals with 2 days of VD, indicating that 2 days of VD saturates synaptic AMPARs contents and occludes LTP. Intact: n = 7, VD: n = 7. Scale bars are as indicated. *Statistical difference (Student's t test). Error bars indicate ± SEM.

(C) (Left) Synaptic responses from layer 4 to layer 2/3 pyramidal neurons at P25 infected with GFP-GluR1 expressing virus at P23 and noninfected neurons of juvenile rats exposed to VD from P21. Note no difference of rectification between infected and noninfected

neurons, indicating no further delivery of GluR1 after 2 days of VD. (Right) Graph of average RI of neurons expressing GFP-GluR1 (green), normalized to RI value of nearby noninfected cells (white). n = 7. Scale bars are as indicated. Note that there was no statistical difference.
Error bars indicate ± SEM.
See also Figure S2.

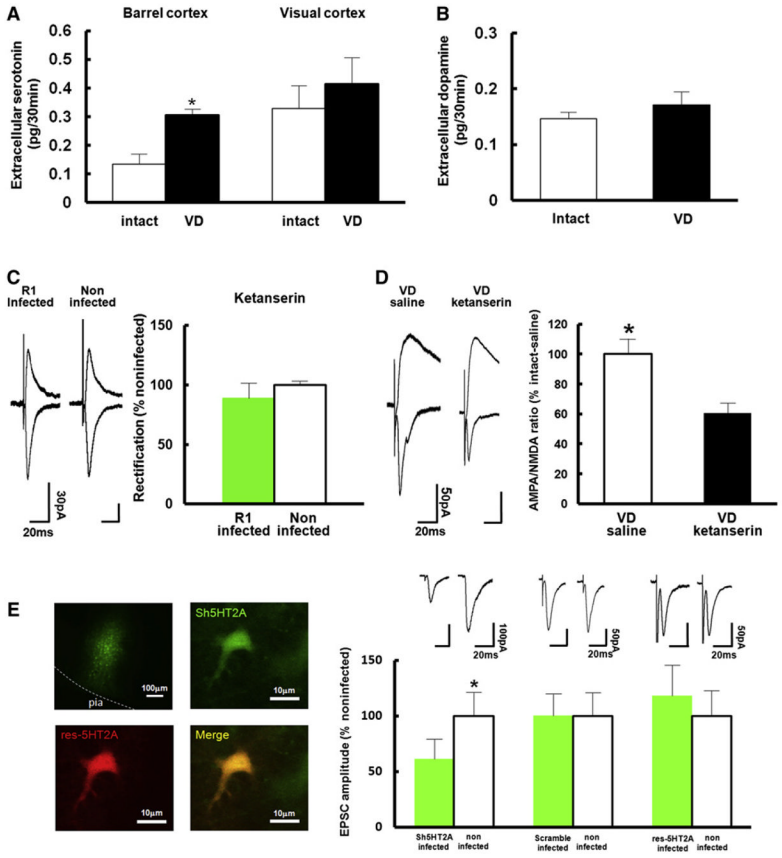

Figure 3. Serotonin Mediates VD-Driven Synaptic GluR1 Delivery in the Juvenile Rat Barrel Cortex

(A) Extracelluar serotonin levels in the layer 2/3 of the barrel cortex and the visual cortex of rats housed under control conditions (white) or VD (black) was measured by in vivo microdialysis. VD increased extracellular serotonin levels in layer 2/3 of the barrel cortex but not of the visual cortex. Barrel cortex; intact: n = 8, VD: n = 6, visual cortex; intact: n = 6, VD: n = 5. *Statistical difference ($p < 0.05$, Student's t test).

(B) Extracelluar dopamine levels in the layer 2/3 of the barrel cortex of rats with intact (white) and sutured eyes (black) was measured with in vivo microdialysis. VD did not increase extracellular dopamine levels in the layer 2/3 of the barrel cortex. Intact: n = 8, VD: n = 6. Note that there was no statistical difference.

(C) (Left) Synaptic responses from layer 4 to layer 2/3 pyramidal neurons infected with virus expressing GFP-GluR1 and noninfected neurons of juvenile VD rats (P21–P23) injected with ketanserin. Note no difference of rectification between infected and noninfected neurons. (Right) Graph of average RI of neurons expressing GFP-GluR1 (green), normalized to RI value of nearby noninfected cells (white). n = 8. Scale bars are as indicated. Note that there was no statistical difference.

(D) Graph of A/N ratio of VD rats (P21–P23) injected with ketanserin normalized to that of VD rats injected with saline. Note that A/N ratio of VD rats injected with saline (white) was larger than that of VD rats injected with ketanserin (black), suggesting that VD-induced synaptic endogenous AMPARs delivery is mediated by serotonin signaling. n = 7. Scale bars are as indicated. *Statistical difference ($p < 0.05$, Student's t test).

(E) (Left) Pictures of tissue expressing Sh5HT2A (upper left) and neurons expressing Sh5HT2A (upper right), res-Sh5HT2A (lower left), and Sh5HT2A+res-Sh5HT2A (lower right). (Top right) Synaptic responses from layer 4 to layer 2/3 pyramidal neurons infected

with virus (expressing Sh5HT2A, a scramble construct, and Sh5HT2A+res-Sh5HT2A) and noninfected neurons of juvenile VD rats (P21–P23). Note knock down of the expression of 5HT2A reduced AMPA transmission in juvenile VD rats. This effect was rescued by the coexpression of res-Sh5HT2A. (Bottom Right) Graph of average amplitude of AMPA transmission of infected neurons (expressing Sh5HT2A, a scramble construct, and Sh5HT2A+res-Sh5HT2A) and noninfected neurons of VD rats. AMPA EPSC amplitude of infected neurons was normalized to those of noninfected neurons. n = 8 (Sh5HT2A), n = 10 (scramble), n = 8 (Sh5HT2A+res-Sh5HT2A). Scale bars are as indicated. *Statistical difference ($p < 0.05$, Wilcoxon nonparametric test).
Error bars indicate ± SEM.
See also Figure S3.

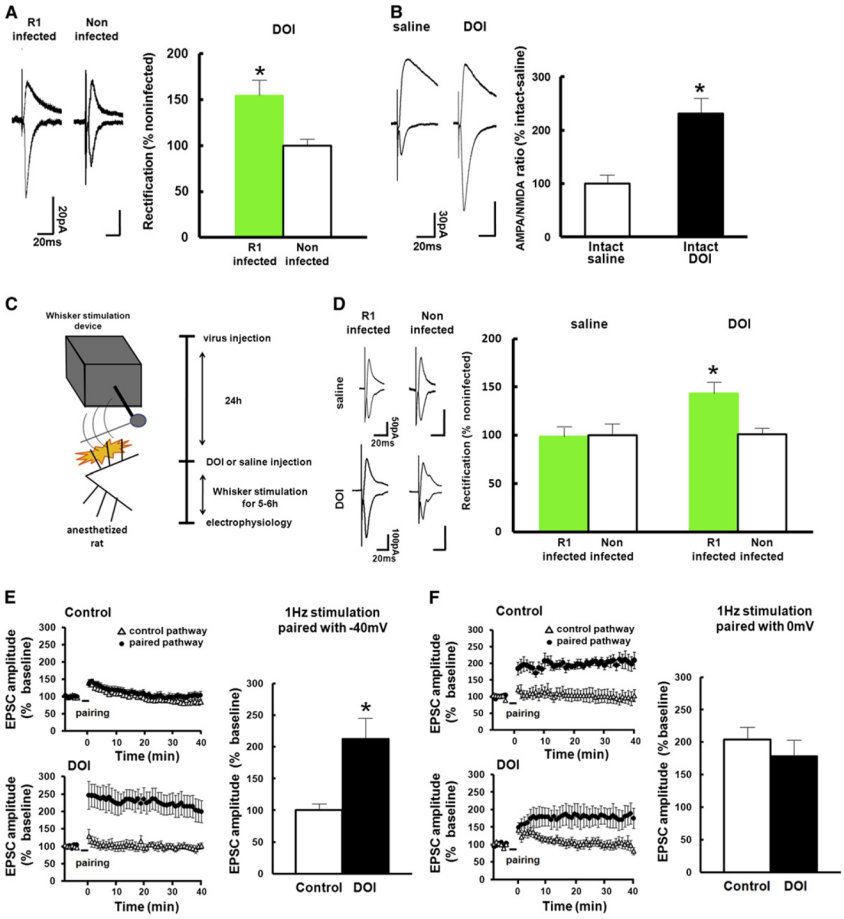

Figure 4. Serotonin Facilitates Synaptic GluR1 Delivery

(A) (Left) Synaptic responses from layer 4 to layer 2/3 pyramidal neurons infected with GFP-GluR1 expressing virus and noninfected neurons of juvenile intact rats (expression during P21–P23) injected with DOI. Note increase of rectification in infected neurons compared with noninfected neurons. (Right) Graph of average RI of neurons expressing GFP-GluR1 (green), normalized to RI value of nearby noninfected cells (white). n = 8. Scale bars are as indicated. *Statistical difference ($p < 0.05$, Student's t test). Error bars indicate ± SEM.

(B) Graph of A/N ratio of intact rats injected with DOI normalized to that of intact rats injected with saline. Note that A/N ratio of intact rats injected with DOI (black) was larger than that of intact rats injected with saline (white), suggesting that increase of serotonin facilitates synaptic endogenous AMPARs delivery. Saline: n = 9, DOI: n = 8. Scale bars are as indicated. *Statistical difference ($p < 0.05$, Student's t test). Error bars indicate ± SEM.

(C) Experimental protocol (see text and Experimental Procedures).

(D) (Left) Synaptic responses from layer 4 to layer 2/3 pyramidal neurons infected with GFP-GluR1 expressing virus and noninfected neurons of juvenile intact rats with mechanical stimulation of whiskers in the presence or absence of DOI. Note increase of rectification in infected neurons compared with noninfected neurons of animals with DOI but not without DOI. (Right) Graph of average RI of neurons expressing GFP-GluR1 (green), normalized to RI value of nearby noninfected cells (white). n = 8. Scale bars are as indicated. *Statistical difference ($p < 0.05$, Student's t test). Error bars indicate ± SEM.

(E) Synaptic plasticity was induced by pairing 1 Hz stimulation (3 min) with postsynaptic potential at −40 mV with (bottom left) or without DOI (top left). The EPSC amplitude was

normalized to the average baseline amplitude before pairing. (Right) Mean amplitude between 30 and 40 min after induction was normalized to base line amplitude. Note that this protocol induced LTP in the presence of DOI (black), while no potentiation was observed in the absence of DOI (white). Control: n = 17, DOI: n = 8. *Statistical difference ($p < 0.05$, Student's t test). Error bars indicate ± SEM.

(F) Synaptic plasticity was induced by pairing 1 Hz stimulation (3 min) with postsynaptic potential at 0 mV with (bottom left) or without DOI (top left). The EPSC amplitude was normalized to the average baseline amplitude before pairing. (Right) Mean amplitude between 30 min and 40 min after induction was normalized to base line amplitude. Note that this protocol induced LTP both with (black) and without DOI (white). Control: n = 5, DOI: n = 7. Note that there was no statistical difference. Error bars indicate ± SEM.

See also Figure S4.

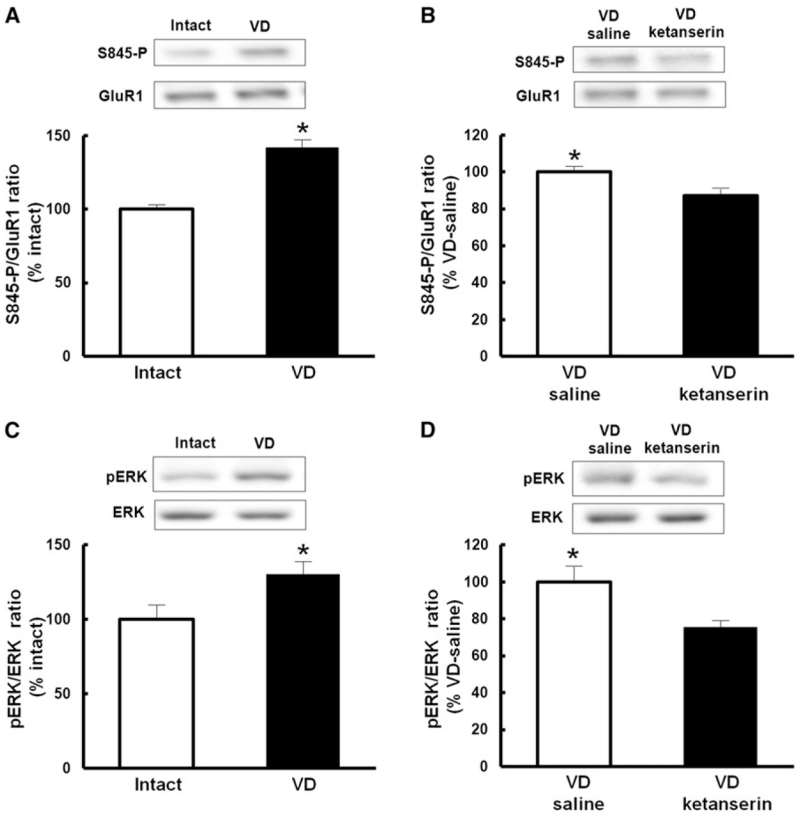

Figure 5. Signaling Pathways of Serotonin-Induced Facilitation of Synaptic GluR1 Delivery

(A) VD increased phosphorylation of Ser845 of GluR1. The amount of GluR1 was used as a reference for the quantitative analysis. Phosphorylation level of VD rats was normalized to that of intact rats. n = 6 (intact), n = 5 (VD).

(B) Ketanserin prevented VD-induced increase of phosphorylation at Ser845 of GluR1. The amount of GluR1 was used as a reference for the quantitative analysis. Phosphorylation level of VD animals with ketanserin was normalized to VD animals with saline. n = 9.

(C) VD activated ERK (p42). Note that phospho-ERK was increased in VD rats compared with intact animals. The amount of total ERK was used as a reference for the quantitative analysis. Phosphorylation level of VD animals was normalized to that of intact animals. n = 6 (intact), n = 5 (VD).

(D) Ketanserin prevented VD-induced activation of ERK. Note that VD-induced increase of phospho-ERK was decreased in the presence of ketanserin. The amount of ERK was used as a reference for the quantitative analysis. Phosphorylation level of VD rats with ketanserin was normalized to VD rats with saline. n = 9.

*$p < 0.05$. Student's t test. Error bars indicate ± SEM.

See also Figure S5.

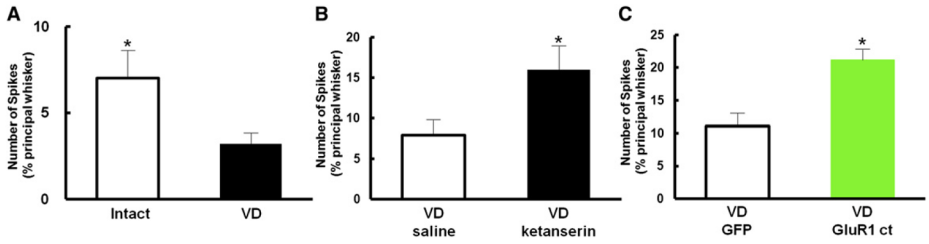

Figure 6. VD Sharpens Functional Whisker-Barrel Map

(A) Responses (number of spikes) in layer 2/3 neurons to deflection of first order surrounding whiskers (S1) are plotted normalized to response in principal whisker. Note that rats with VD (black) showed lower values in S1 than intact rats (white), indicating that map was sharpened in VD rats. n = 14 (intact), n = 14 (VD).

(B) VD rats treated with ketanserin (black) showed higher values in S1 than nontreated VD animals (white), indicating VD-induced sharpening of whisker-barrel map was prevented in the presence of ketanserin. n = 10 (VD with saline), n = 13 (VD with ketanserin).

(C) Rats with VD expressing GFP-GluR1ct (green) showed higher values in S1 than GFP expressing animals (white), indicating a less refined map in GFP-GluR1ct expressing animals. n = 12 (GFP), n = 12 (GFP-GluR1ct).

*Statistical difference (Student's t test). Error bars indicate ± SEM.